

Multilevel Emulation for Stochastic Computer Models with an Application to Large Offshore Windfarms

Jack C. Kennedy*, Daniel A. Henderson and Kevin J. Wilson

School of Mathematics, Statistics and Physics, Newcastle University, UK

July 19, 2022

Abstract

Increasingly, stochastic computer models are being used in science and engineering to predict and understand complex phenomena. Despite the power of modern computing, these simulators are often too computationally costly to be of practical use due to their complexity. Hence the *emulation* of stochastic computer models is a problem of increasing interest. Many stochastic computer models can be run at different levels of complexity, which incurs a trade-off with simulation accuracy. More complex simulations are more expensive to run, but will often be correlated with less complex but cheaper to run versions. We present a heteroscedastic Gaussian process approach to emulation of stochastic simulators which utilises cheap approximations to a stochastic simulator, motivated by a stochastic reliability and maintenance model of a large offshore windfarm. The performance of our proposed methodology is demonstrated on two synthetic examples (a simple, tractable example and a predator-prey model) before being applied to the stochastic windfarm simulator.

Keywords: Emulation; Gaussian Process; Offshore Wind; Multilevel; Stochastic Simulation; Uncertainty Quantification

1 Introduction

Offshore windfarms are becoming a more and more attractive approach to the generation of clean, renewable energy (Hobley 2019). In an effort to make the most of the abundance of offshore wind, offshore windfarms are being composed of more and more turbines. Additionally, turbines are harnessing new technologies and windfarms are being pushed further away from the coast into deep waters. Introducing new technologies to harsh environments induces a large number of uncertainties about, for example, expected lifetimes of critical components,

*Corresponding author j.c.kennedy1@ncl.ac.uk

which ultimately impacts profits. This uncertainty needs to be fully investigated prior to investing time and money into the development of these highly ambitious renewable energy projects.

The uncertainties in windfarms, and other energy projects, fall into two classes: aleatory uncertainties associated with hard-to-predict scenarios such as catastrophic weather events which can severely damage turbines and epistemic uncertainties such as the expected lifetimes of key turbine components and the availability of repair equipment. An approach to investigating these uncertainties is to build a stochastic computer model (a *stochastic simulator*), such as the Athena simulator (Zitrou et al. 2013, 2016), which motivates this article. The Athena simulator is a stochastic simulation of an offshore windfarm, with a focus on the early life of a windfarm. Crucially, Athena can be used to investigate both types of uncertainty. Aleatory uncertainty is investigated by running the simulator multiple times at the same input values. There are hundreds of inputs to the Athena model, but key inputs are often those of lifetime distributions of turbine components. We can investigate epistemic uncertainty by first eliciting a probability distribution over inputs of interest from a group of experts. We then run the simulator at values drawn from this distribution to investigate how input uncertainty induces (epistemic) output uncertainty. A key model output is a time series which tracks the “availability” of a windfarm over time (see Figure 4). The availability of a windfarm at time t is energy output of the windfarm as a proportion of the maximum possible energy output at time t . In our work we compress the availability time series into a single value — the average availability. This is the mean availability over the simulation period. Offshore windfarms reach an availability of around 93% for near shore turbines, but this is reduced for turbines further away from the coast since reaching the turbines for repair is much more difficult (Carroll et al. 2016). Availability is related to a windfarm’s uptime and hence its profitability.

The Athena model is a point processes model which simulates events at discrete times over a time period $[0, T_{max}]$. In our simulations $T_{max} = 5$ (years), which is known as the “early life” of the windfarm. The number of event times is dictated by a tuning parameter Δt , which represents the length of the time step in the simulator. If Δt is too large then we might miss the occurrence of events, which results in an inaccurate simulation. Decreasing Δt gives more accurate simulations but at an increased computational cost. Accurate runs of the Athena simulator can take up to 30 minutes for a windfarm with 200 turbines. The choice of 200 is motivated by the fact that the size of offshore windfarms has been growing quickly and it is likely that we will soon be considering offshore windfarms of this size (Paterson et al. 2018, Vanhellemont & Ruddick 2014). Since the simulator is computationally expensive, it will be highly computationally costly to perform a Monte Carlo type uncertainty analysis in the style of Marrel et al. (2012) to understand the influence of key parameters on windfarm performance. It is common in such scenarios to build a statistical surrogate model — an *emulator* — to replace the simulator in these computations (Gramacy 2020). The theory of emulation of deterministic models is well developed and has been applied to a broad range of scenarios such as calibration (Kennedy & O’Hagan 2001), uncertainty analysis (Kennedy et al. 2006), optimisation (Wilson et al. 2018) and a better understanding of the simulator.

One of the most powerful approaches to emulation (of deterministic simulators) is to construct a Gaussian Process (GP) emulator, although other types of surrogate are available;

see, for example, Goldstein & Rougier (2006), Sudret (2008). Emulators are a “black box” method which are trained on a relatively small number of runs of the computer model (Sacks et al. 1989). Once constructed, emulators produce fast predictions of simulator output at untried inputs. What makes emulators different from other surrogates, is that they also return a quantification of (epistemic) uncertainty attached to the prediction (O’Hagan 2006).

More recently, as *stochastic* simulation has become more prominent, so has the interest in the emulation of stochastic computer simulators, for example, Astfalck et al. (2019), Rocchetta et al. (2018), Boys et al. (2018). There are a variety of approaches to (GP based) emulation of stochastic computer models; see Baker et al. (2020) for a recent overview. One desirable feature of many of these emulators is that they give us not only a mean response but also a quantification of both types of uncertainties in these simulators; the *extrinsic* uncertainty which quantifies our (lack of) knowledge in simulator output, and a prediction of the *intrinsic* uncertainty, that is, the simulator’s level of noise.

Many GP based emulation approaches for stochastic problems rely on large levels of replication. To estimate the mean response of a stochastic simulator, we might apply Stochastic Kriging (SK) to runs of the simulator (Ankenman et al. 2010). For SK it is recommended that we use at least 10 replicates at each design point. If we require a surrogate for the noise, a pair of GP emulators (one for the mean, another for the noise) can be constructed as in Henderson et al. (2009), who use around 1000 replicates per design point. Another input dependent noise formulation is Quantile Kriging (Plumlee & Tuo 2014), which again uses replication – hundreds of replicates are required to model non-Gaussian, input dependent, noise in computer simulators. However, the Athena model can take up to 30 minutes for a single accurate run, thus such levels of replication would make emulation of the Athena model infeasible. It is also likely that for many problems, a simple transformation, such as a log or logit transformation, could remedy any asymmetry in a simulator’s output distribution.

An approach which need not require replication, but still allows for it, is the heteroscedastic GP (HetGP) (Goldberg et al. 1998, Binois & Gramacy 2019). The allure of HetGP is the promise of a full surrogate; joint prediction of the mean response and the level of noise at any input combination. This is possible via a latent variable formulation which jointly models the simulator mean as a GP and the log noise (to ensure positivity) as a GP. As Gramacy (2020) notes, this coupled GP approach provides smooth estimates of the noise at both within sample and out of sample simulator inputs. However, this very flexible approach to emulation may still require prohibitively large sample sizes to properly detect the complex behaviour exhibited by stochastic simulators. For example, Binois et al. (2018) use 500 design points to compare emulators for a one dimensional stochastic simulator.

In the Athena simulator it is simple to change model features to give us cheap approximations to large offshore windfarms. Since these approximations are relatively computationally cheap, it is easy to get enough training data to construct good emulators. If we can build a good emulator for the cheap simulator, and accurately describe its mean, perhaps we can utilise this information to build better emulators for more expensive stochastic computer models.

Using the emulated mean function of a cheap approximation to the expensive simulator has been tackled in the deterministic framework by Kennedy & O’Hagan (2000). The most

popular format is their autoregressive structure for functions (Forrester et al. 2007, Singh et al. 2017, Harvey et al. 2018). They build a well informed emulator for the cheap simulator and use this as a “starting point” for the expensive simulator. The main aim of multilevel emulation is an improved emulation of the (expensive) simulator at a fixed training budget. We aim to extend this to the more complex case of stochastic computer experiments. We believe this is the first serious attempt at producing a full multilevel surrogate model for heteroscedastic simulators. Related work, Stochastic Co-Kriging (SCK), is given by Chen et al. (2017), however their surrogate is a variant on Stochastic Kriging which is aimed at producing a mean response surface and typically requires large amounts of replication. We will focus on a replication-free framework; using the latent variance formulation of HetGP. However we acknowledge that small levels of replication (fewer than 10 replicates) could be a beneficial addition to this work.

The remainder of the article is structured as follows. Section 2 outlines emulation via heteroscedastic Gaussian processes. In Section 3 we motivate and propose stochastic multilevel emulation, which is the key contribution of this article. Simulation studies on a tractable example and a popular predator-prey model are given in Section 4. Section 5 returns to the Athena model where we produce a stochastic multilevel emulator for the motivating problem. Section 6 contains concluding remarks.

2 HetGP

Here we outline HetGP (Binois et al. 2018) to later draw parallels with Stochastic Multilevel (SML) emulation. Suppose we have a complex stochastic simulator, $\eta(\cdot)$. We can model this as a heteroscedastic GP:

$$\begin{aligned}\eta(\cdot) | \lambda^2(\cdot) &\sim \mathcal{GP}\{m(\cdot), C(\cdot, \cdot) + \lambda^2(\cdot)\} \\ \log \lambda^2(\cdot) &\sim \mathcal{GP}\{m_V(\cdot), C_V(\cdot, \cdot) + \lambda_V^2\}.\end{aligned}$$

Here, $m(\cdot)$ and $m_V(\cdot)$ are prior mean functions. These mean functions are typically expressed in a hierarchical form such as $m(\mathbf{x}) = h(\mathbf{x})^T \boldsymbol{\beta}$, where \mathbf{x} is the simulator input, h a collection of simple, deterministic basis functions and $\boldsymbol{\beta}$ are unknown coefficients to be inferred. The mean function on the log-variance $m_V(\cdot)$ is expressed in a similar way, but perhaps with a different choice of $h(\cdot)$ and different values of $\boldsymbol{\beta}$. $\lambda^2(\cdot)$ is the (aleatory) uncertainty of the expensive simulator; the log of this is modelled by a GP which itself has an aleatory uncertainty quantified by λ_V^2 . These noise terms, especially for constant λ , are sometimes referred to as a “nugget” effect (Gramacy & Lee 2012).

Similarly, we parameterise C and C_V , the covariance functions. A common choice of covariance function for computer experiments is the *squared exponential* covariance function, as this imposes the belief that (the moments of) the simulator output are smooth functions of the simulator inputs (Santner et al. 2003). A squared exponential covariance function, for a simulator with K inputs, is of the form

$$C(\mathbf{x}, \mathbf{x}') = \sigma^2 \exp \left\{ (\mathbf{x} - \mathbf{x}')^T D^{-1} (\mathbf{x} - \mathbf{x}') \right\}, \quad (1)$$

where σ^2 is a scale parameter and θ_k are lengthscale parameters. The same form is given to C_V , but the scale (σ_V^2) and lengthscale parameters ($\theta_{k,V}$) can take different values. We then run the simulator n times to obtain training data $\mathcal{D} = \{y_i, \mathbf{x}_i : i = 1, \dots, n\}$, where y_i are single runs/realisations of $\eta(\mathbf{x}_i)$. The hyperparameters, $\Theta = \{\theta_1, \dots, \theta_K, \theta_{1,V}, \dots, \theta_{K,V}, \boldsymbol{\beta}, \boldsymbol{\beta}_V, \sigma, \sigma_V, \lambda_V\}$, can then be inferred and the log variance, $\log \lambda^2(X) = (\log \lambda^2(\mathbf{x}_1), \dots, \log \lambda^2(\mathbf{x}_n))$, at the design points, $X = \{\mathbf{x}_1, \dots, \mathbf{x}_n\}$, can also be estimated (further details in Section 3). Now, conditional on \mathcal{D} , Θ , and $\log \lambda^2(X)$, the posterior predictive distribution of the intrinsic variance at a new input \mathbf{x}^* is

$$\log \lambda^2(\mathbf{x}^*) | \log \lambda^2(X), \mathcal{D}, \Theta \sim \mathcal{N} \{m_V^*(\mathbf{x}^*), C_V^*(\mathbf{x}^*, \mathbf{x}^*) + \lambda_V^2\}.$$

where the posterior moments are found via the conditional normal equations,

$$\begin{aligned} m_V^*(\mathbf{x}^*) &= m_V(\mathbf{x}^*) + C_V(\mathbf{x}^*, X) [C_V(X, X) + \lambda_V^2 I_n]^{-1} (\log \lambda^2(X) - m_V(X)) \\ C_V^*(\mathbf{x}^*, \mathbf{x}^*) &= C_V(\mathbf{x}^*, \mathbf{x}^*) - C_V(\mathbf{x}^*, X) [C_V(X, X) + \lambda_V^2 I_n]^{-1} C_V(X, \mathbf{x}^*) \end{aligned}$$

and I_n is the $n \times n$ identity matrix. Then conditional on the data, and hyperparameters, the posterior predictive distribution of the simulator at an input \mathbf{x}^* is

$$\eta(\mathbf{x}^*) | \Theta, \mathcal{D} \sim \mathcal{N} \{m^*(\mathbf{x}^*), C^*(\mathbf{x}^*, \mathbf{x}^*) + \lambda^{2*}(\mathbf{x}^*)\}.$$

Here, $\lambda^{2*}(\mathbf{x}^*) = \exp\{m_V^*(\mathbf{x}^*)\}$ and $m^*(\mathbf{x}^*)$, $C^*(\mathbf{x}^*, \mathbf{x}^*)$ are also found by the conditional normal equations:

$$\begin{aligned} m^*(\mathbf{x}^*) &= m(\mathbf{x}^*) + C(\mathbf{x}^*, X) [C(X, X) + \lambda^{2*}(X) I]^{-1} (\mathbf{y} - m(X)) \\ C^*(\mathbf{x}^*, \mathbf{x}^*) &= C(\mathbf{x}^*, \mathbf{x}^*) - C(\mathbf{x}^*, X) [C(X, X) + \lambda^{2*}(X) I]^{-1} C(X, \mathbf{x}^*) \end{aligned}$$

where $\mathbf{y} = (y_1, \dots, y_n)$.

In Figure 1 we see an example HetGP emulator for the stochastic simulator $\eta(x) = 5 \sin(4\pi x) + 5x + (1.1 + 4x)\varepsilon$ where $\varepsilon \sim \mathcal{N}(0, 1)$.

Diagnosing problems with the emulation of stochastic computer codes is a difficult problem. Simply observing the fit in Figure 1, the black lines do look like an appropriate description of the stochastic computer model, given the observed model runs (red dots). In this instance we are fortunate enough to know the distribution induced by the simulator; it is clear that the emulator does not provide an accurate representation of the simulator output. It is easy to see that the mean function for the fitted emulator is far too smooth, especially for larger values of x , where the stochasticity is greatest. As a result of this overly smooth fit, the emulated variance is too large in many areas of the input space.

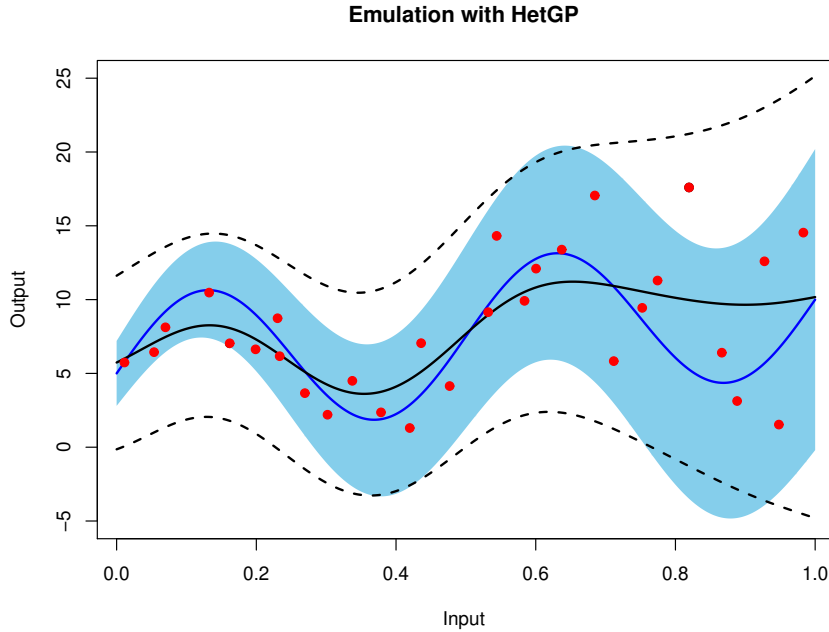


Figure 1: An emulator for $\eta(\cdot)$ constructed via a Heteroscedastic Gaussian process. Solid red points are the outputs from 30 runs of the simulator. Blue line represents the true simulator mean and the blue band represents the mean ± 2 ‘true’ standard deviations. Black solid line represents emulated mean with dashed lines being the emulated mean ± 2 emulated standard deviations.

3 Stochastic Multilevel Emulation

3.1 Motivation and Intuition

We outline our proposed approach to stochastic multilevel (SML) emulation. This approach is quite general and will apply to many stochastic simulators when cheap approximations are available. Many stochastic computer codes have a “complexity parameter”, such as the length of a time step, or granularity of a grid over space, which exchanges simulation accuracy for computational efficiency, examples include Kennedy & O’Hagan (2000) and Le Gratiet & Garnier (2014). The accuracy required frequently comes at a computational cost which severely hinders the size of our computer experiment, limiting the quality of the fitted emulator and future inferences. We aim to exploit such properties in jointly modelling the “cheap” simulator and “expensive” simulator. The outputs from cheap and expensive versions of stochastic simulators will be related. Runs from both versions will be combined to build an overall better emulator.

We will focus on a two level set up; $\eta^C(\cdot)$ is the cheaper simulator and $\eta^E(\cdot)$ is its expensive counterpart. In the motivating example of the Athena model $\eta^C(\cdot)$ is a version of the model with 20 turbines and a time step of $\Delta t = 0.001$. However, we want to infer $\eta^E(\cdot)$, which is a version with time step $\Delta t = 0.0001$ and 200 turbines.

3.2 The Model

Here we will present our stochastic multilevel emulator. We allow for $\eta^E(\cdot)$ to be heteroscedastic but if we believe it is homoscedastic we can replace the non-constant variance with a constant term. Our object of inference is (the distribution of) $\eta^E(\mathbf{x})$, for any \mathbf{x} .

Suppose that the “true” mean of the cheap simulator, $Z_C(\cdot) = \mathbb{E}\{\eta^C(\cdot)\}$, can be modelled by a noise-free (zero nugget) GP with mean function $m_C(\cdot)$ and covariance function $C_C(\cdot, \cdot)$:

$$Z_C(\cdot) \sim \mathcal{GP}(m_C(\cdot), C_C(\cdot, \cdot)).$$

Similarly, the true mean of the expensive simulator ($Z_E(\cdot)$) can be modelled as a GP. However, we cannot ever observe the true mean of the simulator, but some noisy realisation from the simulator $y^C = \eta^C(\mathbf{x})$. We expect that the cheaper simulator is somehow informative for the expensive counterpart and thus, as in Kennedy & O’Hagan (2000), we assume that

$$\eta^E(\cdot) | \rho, \mathbb{E}\{\eta^C(\cdot)\}, \delta(\cdot) = \rho \mathbb{E}\{\eta^C(\cdot)\} + \delta(\cdot)$$

where $\eta^E(\cdot)$ is the expensive stochastic simulator and $\delta(\cdot)$ is a heteroscedastic GP:

$$\begin{aligned} \delta(\cdot) | \lambda_E^2(\cdot) &\sim \mathcal{GP}(m_E(\cdot), C_E(\cdot, \cdot) + \lambda_E^2(\cdot)I) \\ \log \lambda_E^2(\cdot) &\sim \mathcal{GP}(m_V(\cdot), C_V(\cdot, \cdot) + \lambda_V^2 I). \end{aligned}$$

In this formulation, $\rho \in \mathbb{R}$ is a regression parameter and $m_E(\cdot)$, $C_E(\cdot, \cdot)$ are mean and covariance functions for $\delta(\cdot)$. The term $\delta(\cdot)$ serves a dual purpose. Firstly, $\delta(\cdot)$ can be viewed as a discrepancy function; the mean of $\delta(\cdot)$ represents the difference in the mean response of the two simulators, or the loss of accuracy from running cheap simulations (with a large time step/coarse grid). Secondly, $\delta(\cdot)$ describes the stochasticity in the top level simulator. This is a similar structure to that of Bayesian calibration of deterministic computer models (Kennedy & O’Hagan 2001), however we do not observe data from a physical system — but a computer simulator — and we have noise in both sets of observations.

This joint model for the two simulators allows us to borrow information from the cheaper simulator, but is sufficiently flexible to reject a relationship between the two levels if no such relationship exists. Namely, if $\rho = 0$ we recover HetGP.

We express the mean functions in a hierarchical form so that

$$\begin{aligned} m_C(\mathbf{x}) &= h(\mathbf{x})^T \boldsymbol{\beta}^C \\ m_E(\mathbf{x}) &= h(\mathbf{x})^T \boldsymbol{\beta}^E. \end{aligned}$$

We take $h(\cdot)$ to be a set of known, deterministic basis functions with coefficients given by the $\boldsymbol{\beta}$ terms. A typical choice for $h(\cdot)$ is a collection of low order monomials which capture the global variation in the simulator output. A particularly common choice is $h(\mathbf{x}) = (1, \mathbf{x})$ (Fricker et al. 2011, Becker et al. 2012). Hence, the mean functions have the same form, but the particular parameters of these regression functions are allowed to differ.

We will use squared exponential covariance functions so that

$$C_*(\mathbf{x}, \mathbf{x}') = \sigma_*^2 \exp\left\{-(\mathbf{x} - \mathbf{x}')^T D_*^{-1}(\mathbf{x} - \mathbf{x}')\right\}$$

where $* \in \{C, E\}$, $D_* = \text{diag}(\theta_{1,*}^2, \dots, \theta_{K,*}^2)$ is a diagonal matrix containing the correlation lengthscales and σ_* are scale parameters of the covariance functions. The choice of a squared exponential covariance function is imposing the belief that the mean and variance of the simulator are smooth and infinitely differentiable. Intuitively, this means that if an input \mathbf{x} is “close” to another input $\mathbf{x}' \neq \mathbf{x}$ then $E(\eta(\mathbf{x}))$ is also “close” to $E(\eta(\mathbf{x}'))$. Similarly, $\text{Var}(\eta(\mathbf{x}))$ will be close to $\text{Var}(\eta(\mathbf{x}'))$. Note that the choice of squared exponential covariance function is not a requirement for this methodology, the user can specify a different covariance structure as they see fit (Rasmussen 2006).

Hence a hierarchical model for the expensive simulator is as follows:

$$\begin{aligned}\eta^E(\cdot) | \rho, Z_C(\cdot) &= \rho Z_C(\cdot) + \delta(\cdot) \\ \eta^C(\cdot) | Z_C(\cdot) &= Z_C(\cdot) + \mathcal{N}\{0, \lambda_C^2 I_C\} \\ Z_C(\cdot) &\sim \mathcal{GP}\{m_C(\cdot), C_C(\cdot, \cdot)\} \\ \delta(\cdot) | \lambda_E^2(\cdot) &\sim \mathcal{GP}\{m_E(\cdot), C_E(\cdot, \cdot) + \lambda_E^2(\cdot) I_E\} \\ \log(\lambda_E^2(\cdot)) &\sim \mathcal{GP}\{m_V(\cdot), C_V(\cdot, \cdot) + \lambda_V^2 I_E\},\end{aligned}$$

where λ_C is a constant nugget effect for the cheap simulator and λ_V is a constant nugget effect for the latent variance of the expensive simulator, both of which smooth the noisy simulator observations. The I_* are identity matrices of appropriate dimensions. Hence a SML emulator has a similar structure to the standard multilevel emulators presented by Kennedy & O’Hagan (2000), with the addition of a latent variance process ($\lambda_E^2(\cdot)$). We model the log variance as a GP to enforce positivity.

It follows that, conditional on all hyperparameters, $\mathbf{Y} = (\mathbf{Y}^C, \mathbf{Y}^E)^T = (Y_1^C, \dots, Y_{N_C}^C, Y_1^E, \dots, Y_{N_E}^E)^T$ are multivariate normal where N_C and N_E are the number of runs of the cheap and expensive simulators, respectively. That is

$$\begin{pmatrix} \mathbf{Y}^C \\ \mathbf{Y}^E \end{pmatrix} \sim \mathcal{N}_{N_C+N_E} \left\{ \begin{pmatrix} m_C(X^C) \\ \rho m_C(X^E) + m_E(X^E) \end{pmatrix}, \text{Var}(\mathbf{Y}) \right\}$$

where X^C and X^E are the design matrices of the cheap and expensive codes, respectively. Further details of the design are given in Section 3.4 and Section 4.3.

We will now derive the covariance matrix of the response $\mathbf{Y} = (Y_1^C, \dots, Y_{N_C}^C, Y_1^E, \dots, Y_{N_E}^E)$. We express this covariance matrix in block form so that

$$\text{Var}(\mathbf{Y}) = \begin{pmatrix} \text{Var}(\mathbf{Y}^C) & \text{Cov}(\mathbf{Y}^C, \mathbf{Y}^E) \\ \text{Cov}(\mathbf{Y}^E, \mathbf{Y}^C) & \text{Var}(\mathbf{Y}^E) \end{pmatrix}.$$

The auto-covariance of \mathbf{Y}^C is straightforward. This is simply

$$\begin{aligned}\text{Var}(\mathbf{Y}^C)_{i,j} &= \text{Cov}(Y^C(\mathbf{x}_i), Y^C(\mathbf{x}_j)) \\ &= \sigma_C^2 \exp\{-(\mathbf{x}_i - \mathbf{x}_j)^T D_C^{-1}(\mathbf{x}_i - \mathbf{x}_j)\} + \lambda_C^2 \mathbb{I}_{\mathbf{x}_i, \mathbf{x}_j}.\end{aligned}$$

where $\mathbb{I}_{i,j}$ is an indicator function equal to 1 when $i = j$ and 0 otherwise. For the auto-covariance of the expensive simulator, we assume the three summed GPs are all pairwise

independent and that the constant variance of the cheap simulator is independent of the variance of the expensive simulator. Further we assume, for $i \neq j$ that

$$\begin{aligned}\text{Cov}(Z_C(\mathbf{x}_i), \delta(\mathbf{x}_j)) &= 0 \\ \text{Cov}(Z_C(\mathbf{x}_i), \lambda_E^2(\mathbf{x}_j)) &= 0 \\ \text{Cov}(\delta(\mathbf{x}_i), \lambda_E^2(\mathbf{x}_j)) &= 0.\end{aligned}$$

Thus we find that:

$$\begin{aligned}\text{Var}(\mathbf{Y}^E)_{i,j} &= \text{Cov}(Y^E(\mathbf{x}_i), Y^E(\mathbf{x}_j)) \\ &= \text{Cov}(\rho Z_C(\mathbf{x}_i) + \delta(\mathbf{x}_i) + \varepsilon_i^E(\mathbf{x}_i), \rho Z_C(\mathbf{x}_j) + \delta(\mathbf{x}_j) + \varepsilon_j^E(\mathbf{x}_j)) \\ &= \rho^2 \text{Cov}(Z_C(\mathbf{x}_i), Z_C(\mathbf{x}_j)) + \text{Cov}(\delta(\mathbf{x}_i), \delta(\mathbf{x}_j)) + \text{Cov}(\varepsilon_i^E(\mathbf{x}_i), \varepsilon_j^E(\mathbf{x}_j)) \\ &= \rho^2 \sigma_C^2 \exp\{-(\mathbf{x}_i - \mathbf{x}_j)^T D_C^{-1}(\mathbf{x}_i - \mathbf{x}_j)\} \\ &\quad + \sigma_E^2 \exp\{-(\mathbf{x}_i - \mathbf{x}_j)^T D_E^{-1}(\mathbf{x}_i - \mathbf{x}_j)\} + \lambda_E^2(\mathbf{x}_i) \mathbb{I}_{\mathbf{x}_i, \mathbf{x}_j}\end{aligned}$$

where the ε terms are random components of the simulator output.

Finally the cross-covariance is given by

$$\begin{aligned}\text{Cov}(\mathbf{Y}^C, \mathbf{Y}^E)_{i,j} &= \text{Cov}(\mathbf{Y}_i^C, \mathbf{Y}_j^E) \\ &= \text{Cov}(Z_C(\mathbf{x}_i) + \varepsilon_i^C, \rho Z_C(\mathbf{x}_j) + \delta(\mathbf{x}_j) + \varepsilon_j^E(\mathbf{x}_j)) \\ &= \rho \text{Cov}(Z_C(\mathbf{x}_i), Z_C(\mathbf{x}_j)) \\ &= \rho \sigma_C^2 \exp\{-(\mathbf{x}_i - \mathbf{x}_j)^T D_C^{-1}(\mathbf{x}_i - \mathbf{x}_j)\}.\end{aligned}$$

3.3 Prior Specification

Since a Bayesian approach to inference is adopted, we assign priors to all GP hyperparameters. We propose that all parameters are assumed independent *a priori* with the following distributions (where the hyperparameters of the prior are chosen by the user):

$$\begin{aligned}\beta_j^* &\sim \mathcal{N}(m_{j,*}, s_{j,*}^2) \\ \theta_{j,*} &\sim \text{Gamma}(a_{j,*}, b_{j,*}) \\ \sigma_* &\sim \text{Inv-Gamma}(c_{j,*}, d_{j,*}) \\ \lambda_*^2 &\sim \text{Inv-Gamma}(e_{j,*}, f_{j,*}) \\ \rho &\sim \mathcal{N}(m_\rho, s_\rho^2),\end{aligned}$$

where $* \in \{C, E, V\}$. However there is no λ_E since we replace this by a GP to account for heteroscedasticity. We adopt priors over the β_j^* that are very flat, as is often the case in the computer experiments literature (Oakley & Youngman 2017). Hence we take $m_{j,*} = 0$ and $s_{j,*} = 10$. Our priors on θ_* will be fairly weak, but designed to omit very large lengthscales, therefore we take $a_{j,*} = 2$ and $b_{j,*} = 0.5$. Again, fairly weak priors are taken over σ_* ; λ_*^2 and ρ have standard Inv-Gamma priors.

$c_{j,*} = d_{j,*} = 2$ and for λ_*^2 we have $e_j = f_j = 2$. However, in the prior for ρ we are being fairly subjective, we take $m_\rho = 1$ and $s_\rho = 0.5$. This specification expresses the belief that the codes are positively correlated with a high probability; this is a reasonable assertion. If this belief was not held, then there would be little reason to perform a multifidelity computer experiment. This specification is *our* prior specification. In practice, a user can choose a prior that they see suitable.

We will use this same prior specification throughout the document, but where θ_* are vectors (i.e. when the input space has dimension ≥ 2), we will model $\theta_{i,*}$ via independent $Gamma(2, 0.5)$ priors.

3.4 Design

Clearly, the design is an important part of this computer experiment. We want a space filling design on both levels of our experiment, hence we will appeal to a nested Latin Hypercube design. Here, we will use a “one shot” design rather than a more complex, but possibly more efficient, sequential design for simplicity. We generate X^E via a Maximin Latin Hypercube (Morris & Mitchell 1995) (using the `lhs` package in `R`). To create X^C , we *augment* X^E to a larger design which still possesses Latin properties (again via the `lhs` package). Therefore, we have two space filling designs to construct the multilevel emulator.

Non-nested designs have been proposed in the multilevel computer experiments literature, for example Qian & Wu (2008). Such designs treat the points in X^E which are not in X^C as missing data and so data augmentation is performed within a Markov chain Monte Carlo (MCMC) scheme. This can be computationally costly and is easy to avoid with our nested design.

3.5 Posterior Predictive Distribution of Code Output

Within our Bayesian approach, *maximum a posteriori* (MAP) estimates will be used as point estimates of the parameters. In practice, we find the MAP estimates via a numerical optimisation of the log-posterior (up to an additive constant). This is not fully Bayesian, however it is computationally thrifty. We could perform full Bayesian inference via MCMC, however Kersting et al. (2007) note a full Bayes analysis is very computationally expensive for standard Gaussian Process regression problems, let alone our more complicated variant.

Conditional on point (MAP) estimates, and estimates of the log variance at the design points, prediction of the log variance is the same as for HetGP, that is, Gaussian with mean

$$m_V^*(\mathbf{x}) = m_V(\mathbf{x}) + C_V(\mathbf{x}, X^E) \{C_V(X^E, X^E) + \lambda_V^2 I_E\}^{-1} (\log(\lambda_E^2(X^E)) - m_V(X^E))$$

and variance

$$v_V^*(\mathbf{x}) = C_V(\mathbf{x}, \mathbf{x}) + \lambda_V^2 - C_V(\mathbf{x}, X^E) \{C_V(X^E, X^E) + \lambda_V^2 I_E\}^{-1} C_V(X^E, \mathbf{x}).$$

Prediction of the simulator mean at input \mathbf{x} is more complex, but is a natural extension of the posterior predictive mean of a two-level code given in Kennedy & O’Hagan (2000).

Having observed code outputs Y^C , Y^E at design points X^C , X^E , our design matrix is

$$H = \begin{pmatrix} h(\mathbf{x}_1^C)^T & 0 \\ \vdots & \vdots \\ h(\mathbf{x}_{N_c}^C)^T & 0 \\ \rho h(\mathbf{x}_1^E)^T & h(\mathbf{x}_1^E)^T \\ \vdots & \vdots \\ \rho h(\mathbf{x}_{N_E}^E)^T & h(\mathbf{x}_{N_E}^E)^T \end{pmatrix}$$

and hence the posterior distribution for a new input, conditional on a point estimate of the hyperparameters, is Gaussian with mean

$$m^*(\mathbf{x}) = h_0(\mathbf{x})^T \boldsymbol{\beta} + t^T(\mathbf{x}) \text{Var}(\mathbf{Y})^{-1}(Y - H\boldsymbol{\beta})$$

and variance

$$V^*(\mathbf{x}) = V(\mathbf{x}) - t^T(\mathbf{x}) \text{Var}(\mathbf{Y})^{-1} t(\mathbf{x}).$$

where

$$\begin{aligned} h_0(\mathbf{x}) &= (\rho h(\mathbf{x})^T, h(\mathbf{x})^T) \\ \boldsymbol{\beta} &= (\boldsymbol{\beta}^C, \boldsymbol{\beta}^E)^T \\ t^T(\mathbf{x}) &= (\rho \text{Cov}(Z_C(\mathbf{x}), Z_C(X^C)), \rho^2 \text{Cov}(Z_C(\mathbf{x}), Z_C(X^E) + \text{Cov}(\delta(\mathbf{x}), \delta(X^E)))) \\ V(\mathbf{x})_{i,j} &= \rho^2 C_C(\mathbf{x}_i, \mathbf{x}_j) + C_E(\mathbf{x}_i, \mathbf{x}_j) + \lambda_E^2(\mathbf{x}_i) \mathbb{I}_{i,j}. \end{aligned}$$

4 Simulation Studies

4.1 Emulator Comparison

Before we apply SML to the Athena model, we first perform two simulation studies. The first simulation study is on a simple tractable example, and the second is on a more challenging example, the stochastic Lotka-Volterra model. We use the Stochastic Lotka-Volterra model as it has several features in common with the Athena windfarm simulator, but is much less complex.

To compare multilevel emulation with HetGP we can use the mean squared error,

$$\text{MSE} = \frac{1}{N_{test}} \sum_{j=1}^{N_{test}} (y(\mathbf{x}_j) - \hat{y}(\mathbf{x}_j))^2,$$

where $y(\mathbf{x}_j)$ are a set of N_{test} unseen simulator outputs (or possibly the known mean, as in Section 4.2.2) with unseen inputs \mathbf{x}_j and $\hat{y}(\mathbf{x}_j)$ are predictions of the mean simulator output at each \mathbf{x}_j . Another suitable summary, especially since we emulate both the simulator mean and variance, would be a proper scoring rule. We shall use the scoring rule given in Equation

Experiment	HetGP	SML
(a)	30 expensive runs	29 expensive + 100 cheap runs
(b)	30 expensive runs	29 expensive + 50 cheap runs
(c)	10 expensive runs	9 expensive + 100 cheap runs
(d)	10 expensive runs	9 expensive + 50 cheap runs

Table 1: Design strategies for comparing HetGP and SML on the tractable example.

(27) of Gneiting & Raftery (2007). For distribution \mathcal{P} , with mean μ and standard deviation σ , the score for this rule is $S(y, \mathcal{P}) = -((\mu - y)/\sigma)^2 - \log \sigma^2$, where y is the quantity we wish to forecast. In our case, y will be the output from a run of the simulator of interest and \mathcal{P} is the posterior predictive distribution of the simulator output. This scoring rule has recently been used by others when comparing different emulators for stochastic simulators (Binois et al. 2018, Baker et al. 2019). For this particular scoring rule, a bigger score is better.

4.2 Tractable Example

We will emulate two simple, stochastic simulators:

$$\begin{aligned}\eta^E(x) &= 5(\sin(x) + x) + (1.1 + 4x)\varepsilon^E \\ \eta^C(x) &= 5\sin(x) + 0.5\varepsilon^C,\end{aligned}$$

where the $\varepsilon^* \sim \mathcal{N}(0, 1)$ for $* \in \{C, E\}$. It is clear that the above simulators are related via $\sin(x)$ and therefore $\eta^C(\cdot)$ should tell us something useful about $\eta^E(\cdot)$. However, the variance component of $\eta^E(\cdot)$ becomes quite large with x — potentially making the simulator quite difficult to emulate, as seen in Figure 1.

4.2.1 Design for the Tractable Example

When building emulators of stochastic computer models, the number of training runs we can make will typically be limited by the available CPU time. Therefore, when building multilevel emulators from scratch, we are forced to trade a small number of runs of the expensive simulator for a relatively large number of runs from the cheap simulator (of course, if data from the cheap simulator is already available, our framework would allow for it to be used). In this simulation study, the simple simulators are virtually instantaneous to run, so we will try a few different experiments where the relative expense of the simulators will change. We will suppose in one set of experiments that the cheap simulator is 100 times quicker than the expensive simulator. We will then see what happens when the cheap simulator is only 50 times quicker. We will also vary the absolute simulation budget; we will allow a set of experiments with a budget equivalent to 30 expensive runs, and another set with a budget equivalent to 10 expensive runs. We therefore have four simulation experiments in this section, which are summarised in Table 1.

We shall run each simulation study 100 times, comparing the MSE and Score of the stochastic multilevel emulator to that of the HetGP emulator. Since in this case we know the exact form of the simulator, we shall compare the MSE and score via:

- (i) The true mean of the simulator ('true' MSE).
- (ii) A randomly generated set of 500×100 data points. Here, the inputs will be 500 equally spaced points on $[0, 1]$, with 100 replicates at each design points. We generate 100 realisations from the expensive simulator at each design point ('empirical MSE').

4.2.2 Results

For each of the experiments outlined above we shall report the number of times (out of 100) that SML outperformed HetGP for each performance summary; see Table 2. We will also report the lower quartile, median and upper quartile of the performance summaries; see Table 3. First we will report the number of times that SML emulation outperformed HetGP for each of the experiments. We aim to minimise MSE and for this particular scoring rule, a higher score is better.

Experiment	MSE (true)	MSE (empirical)	Score
(a)	97	97	86
(b)	98	98	77
(c)	94	94	46
(d)	93	93	32

Table 2: A simple summary of emulation performance showing the number of times SML emulation outperformed HetGP (out of 100) for the simple, tractable simulator.

We see in Table 2 that, in these experiments, the MSE is almost always reduced by incorporating runs from a cheaper simulator. We see a different story for the score – SML provides a worse score than HetGP when the number of expensive runs is 10. However, the MSE is still considerably reduced in these cases as seen in Table 3. This suggests that by trading expensive runs for cheap runs we are losing some information about the stochasticity of the expensive simulator. This was also seen by Baker et al. (2019) when trading stochastic runs for deterministic runs to improve the emulation of stochastic simulators. Also we see that the difference in MSE is much more distinct for the true cases than empirical, however in both cases the MSE is reduced by employing the multilevel emulator.

4.3 The Lotka-Volterra Model

A commonly used stochastic simulator, with fast approximations, is the stochastic Lotka-Volterra model (from hereon in, the Lotka-Volterra model), used to model predator-prey systems.

The Lotka-Volterra model is commonly phrased in terms of rabbits (prey, x_1) and foxes (predators, x_2). In the Lotka-Volterra model, at the time of an event, one of three things can

		MSE (true)	MSE (empirical)	Score
(a)	HetGP	(1.66, 2.54, 3.45)	(12.86, 13.81, 14.99)	(-1912, -1871, -1820)
	SML	(0.42, 0.80, 1.44)	(11.27, 11.73, 12.40)	(-1778, -1690, -1635)
(b)	HetGP	(1.87, 2.74, 4.01)	(12.72, 13.76, 15.09)	(-1903, -1851, -1819)
	SML	(0.40, 1.10, 1.59)	(11.36, 11.74, 12.57)	(-1796, -1677, -1636)
(c)	HetGP	(10.39, 11.13, 13.48)	(21.31, 22.16, 24.50)	(-2226, -2244, -2032)
	SML	(1.28, 2.49, 4.23)	(12.19, 14.39, 15.07)	(-4900, -2349, -1865)
(d)	HetGP	(10.40, 11.23, 13.02)	(21.30, 22.201, 24.05)	(-2252, -2138, -2032)
	SML	(1.24, 2.54, 5.22)	(12.22, 13.51, 16.04)	(-6175, -3080, -2027)

Table 3: Summary of results for tractable example under four different possible budget regimes. Given quantities are (Lower Quartile, Median, Upper Quartile).

happen; prey reproduce ($x_1 := x_1 + 1$), a prey death coupled with a predator reproduction ($x_1 := x_1 - 1$, $x_2 := x_2 + 1$) or a predator death ($x_2 := x_2 - 1$). The events occur in accordance to the hazard vector $h(\mathbf{x}|\mathbf{c}) = (c_1 x_1, c_2 x_1 x_2, c_3 x_2)^T$. The time until the next event is then Exponentially distributed with rate $h_0 = \sum_i h_i(\mathbf{x}|\mathbf{c})$. Exact realisations from the Lotka-Volterra model are available via Gillespie’s algorithm; for further details see Wilkinson (2011).

However, there are several ways to generate (approximate) simulations from the Lotka-Volterra simulator. They all rely on setting some initial state vector $x = (x_1, x_2)$ which changes with time according to some reaction rates $c = (c_1, c_2, c_3)$. Here we will focus on one of the most simple approximate implementations of the Lotka-Volterra model; a Poisson leaping scheme.

4.3.1 Poisson Leaping

Poisson leaping is a simple, approximate method for generating simulations from the Lotka-Volterra model. For a small time period $[t, t + \Delta t]$ it is assumed that the number of times event i occurred follows a $\text{Poisson}(h_i \Delta t)$ distribution (for further details see Golightly & Gillespie (2013)). Decreasing the length of the leap, Δt , increases simulation accuracy at the cost of computation time. For many simulations, it is not clear if there is a “best” leap length.

4.3.2 Multilevel Emulation of the Lotka-Volterra Model

We want to produce an emulator for the Lotka-Volterra model. Our output of interest here will be the average number of predators over the simulation period $[0, T_{\max}]$ and we will vary the three reaction rates in the simulator. We will use multilevel emulation to predict the

mean number of predators over the time period with the cheap simulator being a Poisson leaping scheme with a large time step ($\Delta t = 0.1$), and a corresponding expensive version will have a much smaller time step ($\Delta t = 0.001$).

On average, the smaller time step algorithm takes approximately 100 times longer than the large time step; a substantial computational saving. We also see in Figure 2 that there is large agreement (and very high positive correlation) between the two algorithms when the output is relatively small, but when the mean number of prey is more than around 3000, any relationship is not obvious.

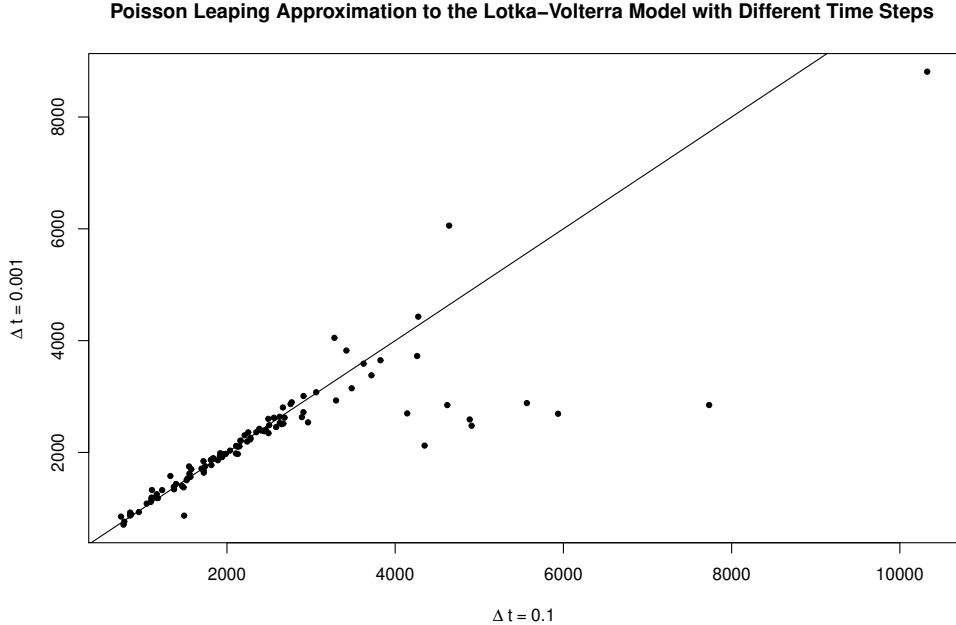


Figure 2: Comparing the output from Poisson leaping with a small ($\Delta t = 0.001$) and large ($\Delta t = 0.1$) time step. Each point represents the sample mean of 10 realisations of the average number of prey over the time period with a particular set of reaction constants. The black line represents the unit diagonal.

4.3.3 Results for the Lotka–Volterra Model

We shall evaluate the methods (SML and HetGP) here via repeated simulation. We will perform 100 simulation studies from the Lotka–Volterra model and investigate the (out of sample) mean squared error as well as the score (again, computed using out of sample data). We cannot report the ‘true’ MSE here since it is not available, as will be the case for many simulators of interest. We shall emulate the log average number of prey over the time period (to ensure positivity of predictions). For these experiments, we shall assume a computational budget which allows for 40 expensive runs. To build the multilevel emulator, we exchange just one expensive run for 100 runs from the cheap simulator. This should allow us to learn as much as possible about the stochasticity of the expensive simulator and keep the cost of inference and prediction relatively low.

Figure 3 compares a HetGP emulator and an SML emulator. We see in the plot that the mean functions, although similar, have some differences. For instance, HetGP gives a fit (on the log scale) which is closer to a straight line than the multilevel emulator. We also see, especially when c_3 is small, that the variances are quite different. It is not obvious which fit is best. Hence to test the methods we rely on assessing out-of-sample performance on an independently generated test data set.

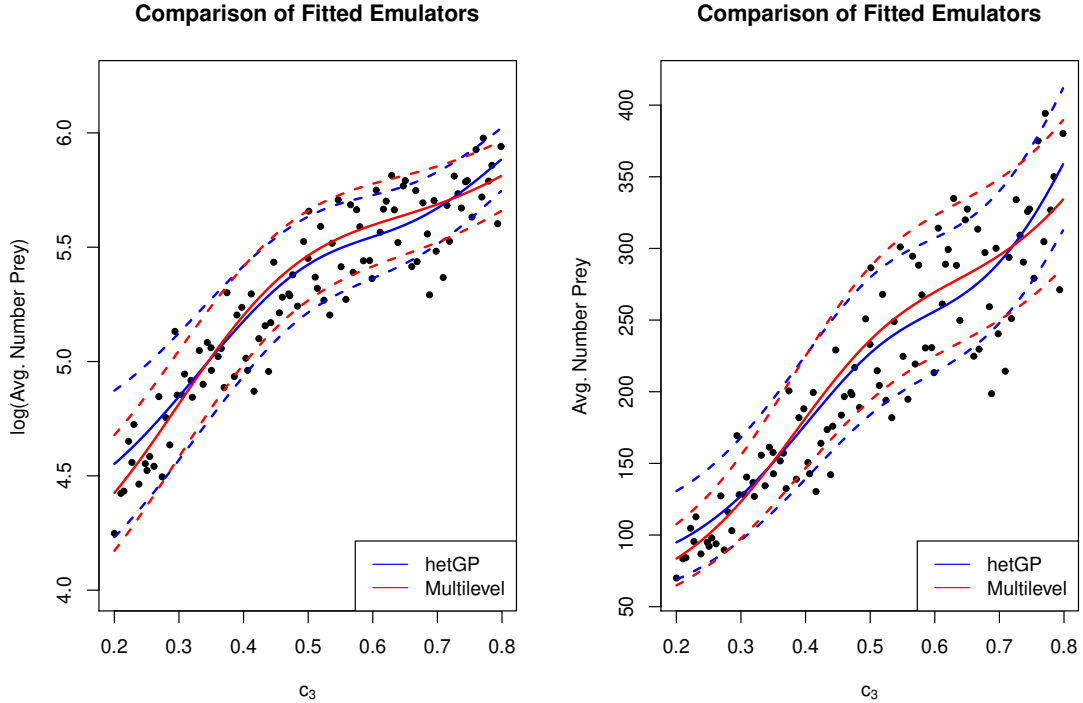


Figure 3: A HetGP emulator and Stochastic Multilevel Emulator for the Lotka-Volterra model with c_1 fixed at 0.5 and c_2 fixed at 0.0025. The left plot shows the original emulators and the right has the output transformed to the original scale. The black points are realisations from an independent test set of data (where all the c_i were varied).

For the Lotka-Volterra model with different leap lengths, we obtain the following results. The MSE was smallest for SML emulation on 95 occasions and a larger score was obtained on 94 occasions. Jointly, the MSE and score were favourable on 90% of the simulation experiments.

We see in Table 4 a numerical summary of the performance of each emulation approach. For this experiment, a validation set of data was generated, consisting of 100 design points and one run of the simulator at each design point. We see quite clearly that multilevel emulation is favourable in this case, although the experiment conducted was much smaller than in the tractable example, so the evidence is perhaps less convincing.

MSE (empirical) / 10^{-2}			Score
HetGP	(1.15, 1.35, 1.57)		(2.13, 2.79, 2.88)
SML	(0.96, 1.13, 1.29)		(2.54, 3.44, 3.58)

Table 4: (LQ, Median, UQ) of performance metrics for HetGP and SML emulators for the Lotka-Volterra model. 100 simulation studies were carried out with a computational budget equivalent to 40 expensive runs.

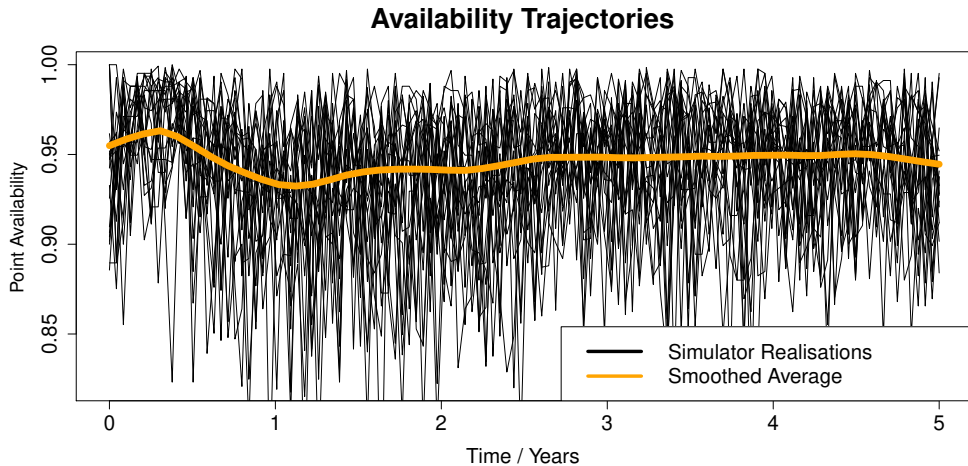


Figure 4: A collection of 10 availability trajectories (black lines) over the first 5 years of a windfarm’s operational life. The orange line represents a smoothed average of the trajectories.

5 Multilevel Emulation of the Athena Simulator

We now return to the motivating example for SML; the Athena model. Athena is a large point-process model. Simulations are implemented via MATLAB with a large number of inputs. Many inputs are parameters of lifetime distributions of components in wind turbines, but others, for instance, relate to the availability of repair equipment.

The Athena model was also developed with *short term* wind farm performance in mind. In our simulations, we simulate the first 5 years of the windfarm’s operational life. This time period is usually called “early life”, which typically coincides with the warranty period of key sub-assemblies (Zitrou et al. 2016) and is critical to meeting availability targets.

Some sample trajectories of the model are shown in Figure 4. The availability over the time period, for a single run, is simply the average availability of that run. For the cheap version of the simulator, trajectories are very coarse compared to the expensive runs. This results in the variance of the availability being overly inflated. Further, since the Athena simulator is a point-process, by taking large time steps we frequently “miss” the occurrence of events, thus the smallest feasible time step is favoured.

Two ways to alter the speed of the Athena simulator are (i) changing the size of the time

step, (ii) changing the number of turbines in the windfarm.

Of course, changing each of the parameters will somehow impact the output of the simulator. Experimentation suggests that increasing the size of the time step not only systematically reduces a windfarm’s availability, but also inflates the intrinsic variance. A system with a small number of turbines (say, 20 turbines) runs much faster than a system with a much larger number (say, 200). We aim to learn about the behaviour of a 200 turbine windfarm, but a 20 turbine windfarm will give us a useful insight into a larger system. Similarly, a fast, but coarse, simulation will give us information about a slow, but accurate, simulation (as in Section 4.3). If we can produce a good emulator for a 200 turbine windfarm simulator then we should, in theory, be able to perform otherwise computationally intensive tasks such as uncertainty analysis for many future offshore wind projects.

We will construct emulators over a 6 dimensional input space which is summarised in Table 5. The design points are chosen via the nested Latin Hypercube structure described in Section 3.4. To construct the emulator, we standardise the inputs by subtracting the sample means and then dividing by the sample standard deviations, we refer to these transformed inputs as x_i^* .

Input	Name	Range
x_1	Learning Rate	(1.5, 10)
x_2	Cable Failure Rate	(10^{-4} , 1)
x_3	Cable Repair Time	(10^{-1} , 10)
x_4	Gearbox TTWO	(10^{-1} , 1.5)
x_5	Generator TTWO	(10^{-1} , 1.5)
x_6	Frequency Converter TTWO	(10^{-1} , 1.5)

Table 5: Summary of the six Athena inputs. TTWO = “time to wear out”.

Choosing the sample size for a stochastic computer experiment is not an easy task. However, it seems reasonable that we should exceed the 10 points per input rule of thumb suggested by Loeppky et al. (2009). For this experiment, we generated 200 cheap training points and 80 expensive training points. The expensive simulator takes approximately 26 minutes per run. The cheap simulator takes around 15 seconds per run. The more expensive simulator here takes more than 100 times longer to run than the cheaper counterpart. To build the multilevel emulator, we exchanged 2 expensive runs for the 200 cheap runs. An additional 500 runs of the model were generated to act as validation data, with inputs chosen via Maximin Latin hypercube.

We then constructed the two types of emulator. Based on the set of 500 independently generated validation data, the MSE for HetGP was 0.385 whereas SML achieved an MSE of 0.352. The score for HetGP was -1317.485 and for SML the score was -113.362 . Hence, SML achieves better MSE and score here than HetGP for the Athena model. Additionally, we estimated $\hat{\rho} = 0.817$ for this example.

5.1 Emulator Validation

In order to check the validity of the emulators, we will implement some of the graphical diagnostics proposed by Bastos & O'Hagan (2009). Since we model the outputs of the simulators by a Gaussian process, the Studentised residuals should form a random sample from a $\mathcal{N}(0, 1)$ distribution (approximately). If the posterior mean and variance are well suited to the simulator, the validation data should lie in a horizontal band, centred at 0, with approximately 95% of points in the interval $(-2, 2)$. We can also compare empirical quantiles of the Studentised residuals against theoretical quantiles – we do this via coverage plots (comparing the proportion of Studentised validation samples in the interval $(\Phi^{-1}(\alpha/2), \Phi^{-1}(1 - \alpha/2))$ against the expected proportion).

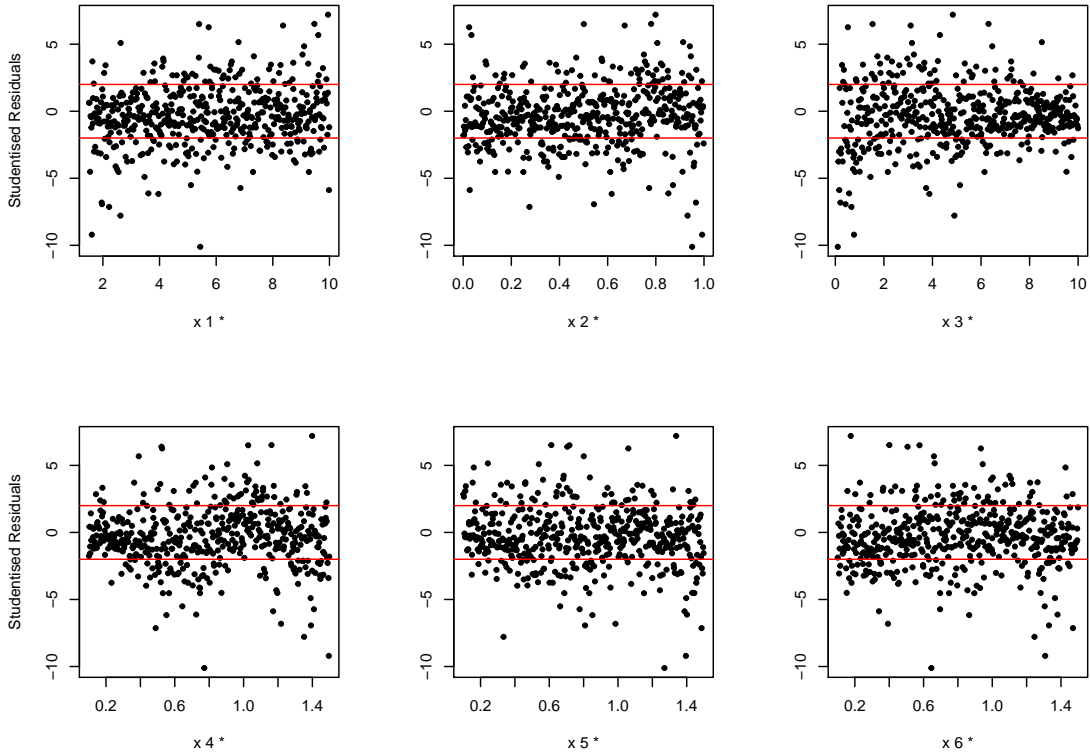


Figure 5: Studentised residual plots for HetGP, based on 500 “unseen” validation points. Solid red lines are at ± 2 .

We see in Figure 5 that the magnitude of Studentised residuals for HetGP can be very large and far more residuals than we would expect are outside the range $(-2, 2)$: 31.2%. For SML (Figure 6) the residuals are slightly heavy tailed: 12.2% of residuals are outside of $(-2, 2)$, slightly more than expected but a clear improvement over HetGP. We also see that the variances of the Studentised residuals are non-constant for HetGP, most noticeably in the third input. Our multilevel emulator appears to have resolved this problem. The coverage plots (Figure 7) also show that the Gaussian assumption is more plausible for the SML emulator than HetGP.

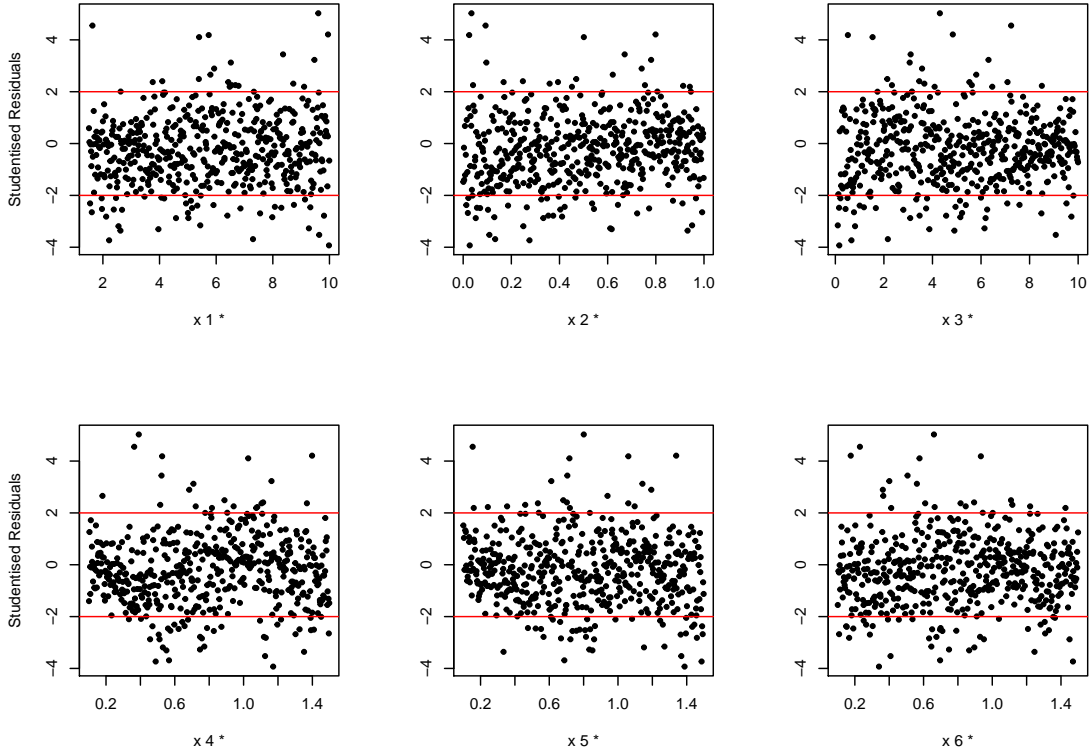


Figure 6: Studentised residual plots for SML emulation, based on 500 “unseen” validation points. Solid red lines are at ± 2 .

6 Conclusions & Further Work

We have presented a novel application of multilevel emulation to stochastic simulators, which was first presented for deterministic computer codes by Kennedy & O’Hagan (2000).

We have shown that this approach can be favourable for both a tractable example, a fairly simple, but “genuine” simulator and also a problem of practical interest. On the downside, prediction and inference with multilevel modelling is slower, since such computations are $\mathcal{O}(N^3)$ where N is the size of the design. In HetGP (without replication) N is the number of design points, whereas in multilevel emulation $N = N_E + N_C$, and N_C is typically fairly large. We however believe that the benefits of multilevel emulation, increased emulator performance at a fixed training budget, may outweigh this extra cost.

Future work could involve using (small amounts of) replication in the cheap simulator so that N_C is smaller. Interestingly, the MSE/score did not improve much in Table 3 when an additional 50 cheap runs were added. Perhaps these 50 runs would have been better used on replication in the cheap simulator to improve the efficiency of prediction and inference with SML emulation.

This new approach to emulation also poses a design question: how should we split the computational budget between cheap and expensive runs to build the best possible emulator?

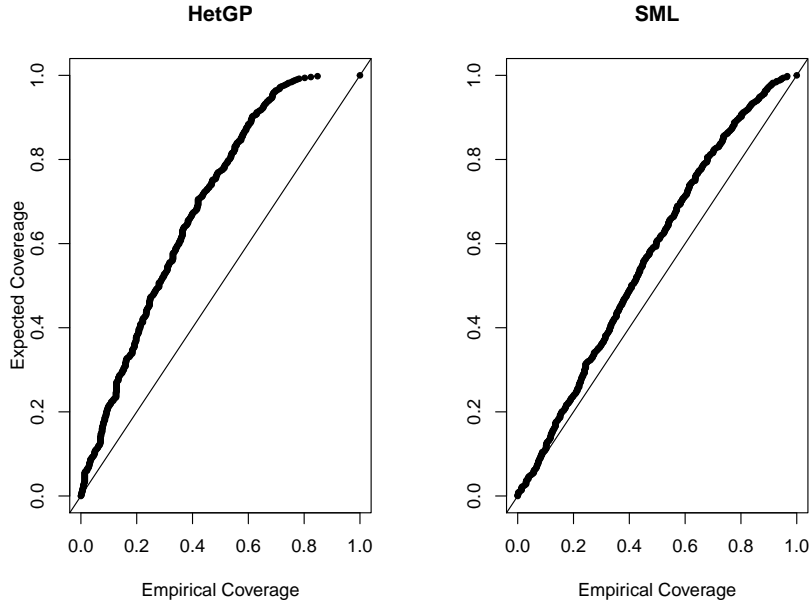


Figure 7: Out of sample coverage plots, based on the set of 500 validation points.

For our experiments, we typically exchanged the fewest number of expensive runs possible. This was so that we could learn as much about the latent variance process as possible and to avoid computational issues associated with large N_C . Of course a rule for the design might be highly dependent on the problem. It is likely to depend on how correlated the expensive and cheap runs are, but should also account for the relative cost of each simulator. It might not be the case that a “one shot” design rule is simple to construct. Hence a sequential design could be a powerful approach. Sequential design of multilevel deterministic computer codes is addressed by Le Gratiet & Cannamela (2015). Further, sequential designs which balance replication and exploration in stochastic computer codes, to create cheaper emulators, have been presented by Binois et al. (2019).

Another interesting problem, which we have not addressed here, is linking the stochasticity of the two simulators. Our approach aimed to build better surrogates for stochastic simulators by constructing a well-informed mean function. It could be the case that the variance of each simulator is somehow related. Perhaps a good understanding of the stochasticity in a cheap simulator could deliver an improved understanding of stochasticity in the expensive simulator. It would be interesting to see if this could be developed in a computationally efficient manner.

Acknowledgements

The authors would like to thank the Engineering and Physical Sciences Research Council for JCK’s studentship, and the Centre of Energy Systems Integration, grant number *EP/P001173/1* for further financial support.

We would also like to thank Professor Tim Bedford and Professor Lesley Walls of the Uni-

versity of Strathclyde for discussions about the Athena simulator and access to the Athena simulator.

References

Ankenman, B., Nelson, B. L. & Staum, J. (2010), 'Stochastic Kriging for simulation meta-modeling', *Operations Research* **58**(2), 371–382.

Astfalck, L., Cripps, E., Gosling, J. & Milne, I. (2019), 'Emulation of vessel motion simulators for computationally efficient uncertainty quantification', *Ocean Engineering* **172**, 726–736.

Baker, E., Barbillon, P., Fadikar, A., Gramacy, R. B., Herbei, R., Higdon, D., Huang, J., Johnson, L. R., Ma, P., Mondal, A., Pires, B., Sacks, J. & Sokolov, V. (2020), 'Stochastic Simulators: An Overview with Opportunities'.

Baker, E., Challenor, P. & Eames, M. (2019), 'Predicting the Output From a Stochastic Computer Model When a Deterministic Approximation is Available', *arXiv e-prints* p. arXiv:1902.01290.

Bastos, L. S. & O'Hagan, A. (2009), 'Diagnostics for Gaussian process emulators', *Technometrics* **51**(4), 425–438.

Becker, W., Oakley, J., Surace, C., Gili, P., Rowson, J. & Worden, K. (2012), 'Bayesian sensitivity analysis of a nonlinear finite element model', *Mechanical Systems and Signal Processing* **32**, 18–31.

Binois, M. & Gramacy, R. B. (2019), *hetGP: Heteroskedastic Gaussian Process Modeling and Design under Replication*. R package version 1.1.1.
URL: <https://CRAN.R-project.org/package=hetGP>

Binois, M., Gramacy, R. B. & Ludkovski, M. (2018), 'Practical heteroscedastic Gaussian process modeling for large simulation experiments', *Journal of Computational and Graphical Statistics* **27**(4), 808–821.

Binois, M., Huang, J., Gramacy, R. B. & Ludkovski, M. (2019), 'Replication or exploration? sequential design for stochastic simulation experiments', *Technometrics* **61**(1), 7–23.

Boys, R. J., Ainsworth, H. F. & Gillespie, C. S. (2018), 'Bayesian inference for a partially observed birth–death process using data on proportions', *Australian & New Zealand Journal of Statistics* **60**(2), 157–173.

Carroll, J., McDonald, A. & McMillan, D. (2016), 'Failure rate, repair time and unscheduled O&M cost analysis of offshore wind turbines', *Wind Energy* **19**(6), 1107–1119.

Chen, X., Hemmati, S. & Yang, F. (2017), Stochastic co-Kriging for steady-state simulation metamodeling, in 'Proceedings of the 2017 Winter Simulation Conference', IEEE Press, p. 136.

Forrester, A. I., Sóbester, A. & Keane, A. J. (2007), 'Multi-fidelity optimization via surrogate modelling', *Proceedings of the Royal Society A: Mathematical, Physical and Engineering sciences* **463**(2088), 3251–3269.

Fricker, T. E., Oakley, J. E., Sims, N. D. & Worden, K. (2011), 'Probabilistic uncertainty analysis of an FRF of a structure using a Gaussian process emulator', *Mechanical Systems and Signal Processing* **25**(8), 2962–2975.

Gneiting, T. & Raftery, A. E. (2007), 'Strictly proper scoring rules, prediction, and estimation', *Journal of the American Statistical Association* **102**(477), 359–378.

Goldberg, P. W., Williams, C. K. & Bishop, C. M. (1998), Regression with input-dependent noise: A Gaussian process treatment, in 'Advances in Neural Information Processing Systems', pp. 493–499.

Goldstein, M. & Rougier, J. (2006), 'Bayes linear calibrated prediction for complex systems', *Journal of the American Statistical Association* **101**(475), 1132–1143.

Golightly, A. & Gillespie, C. S. (2013), Simulation of stochastic kinetic models, in 'In Silico Systems Biology', Springer, pp. 169–187.

Gramacy, R. B. (2020), *Surrogates: Gaussian Process Modeling, Design and Optimization for the Applied Sciences*, Chapman Hall/CRC, Boca Raton, Florida.
URL: <http://bobby.gramacy.com/surrogates/>

Gramacy, R. & Lee, H. (2012), 'Cases for the nugget in modelling computer experiments', *Statistics and Computing* **22**(3), 713–722.

Harvey, N. J., Huntley, N., Dacre, H. F., Goldstein, M., Thomson, D. & Webster, H. (2018), 'Multi-level emulation of a volcanic ash transport and dispersion model to quantify sensitivity to uncertain parameters', *Natural Hazards and Earth System Sciences* **18**(1), 41–63.

Henderson, D. A., Boys, R. J., Krishnan, K. J., Lawless, C. & Wilkinson, D. J. (2009), 'Bayesian emulation and calibration of a stochastic computer model of mitochondrial DNA deletions in substantia nigra neurons', *Journal of the American Statistical Association* **104**(485), 76–87.

Hobley, A. (2019), 'Will gas be gone in the United Kingdom (UK) by 2050? An impact assessment of urban heat decarbonisation and low emission vehicle uptake on future UK energy system scenarios', *Renewable Energy* **142**, 695–705.

Kennedy, M. C., Anderson, C. W., Conti, S. & O'Hagan, A. (2006), 'Case studies in Gaussian process modelling of computer codes', *Reliability Engineering & System Safety* **91**(10–11), 1301–1309.

Kennedy, M. & O'Hagan, A. (2000), 'Predicting the output from a complex computer code when fast approximations are available', *Biometrika* **87**(1), 1–13.

Kennedy, M. & O'Hagan, A. (2001), 'Bayesian calibration of computer models', *Journal Of The Royal Statistical Society Series B-Statistical Methodology* **63**, 425–450.

Kersting, K., Plagemann, C., Pfaff, P. & Burgard, W. (2007), Most likely heteroscedastic Gaussian process regression, in 'Proceedings of the 24th international conference on Machine learning', pp. 393–400.

Le Gratiet, L. & Cannamela, C. (2015), ‘Cokriging-based sequential design strategies using fast cross-validation techniques for multi-fidelity computer codes’, *Technometrics* **57**(3), 418–427.

Le Gratiet, L. & Garnier, J. (2014), ‘Recursive co-Kriging model for design of computer experiments with multiple levels of fidelity’, *International Journal for Uncertainty Quantification* **4**(5).

Loeppky, J. L., Sacks, J. & Welch, W. J. (2009), ‘Choosing the sample size of a computer experiment: A practical guide’, *Technometrics* **51**(4), 366–376.

Marrel, A., Iooss, B., Da Veiga, S. & Ribatet, M. (2012), ‘Global sensitivity analysis of stochastic computer models with joint metamodels’, *Statistics and Computing* **22**(3), 833–847.

Morris, M. D. & Mitchell, T. J. (1995), ‘Exploratory designs for computational experiments’, *Journal of Statistical Planning and Inference* **43**(3), 381–402.

Oakley, J. E. & Youngman, B. D. (2017), ‘Calibration of stochastic computer simulators using likelihood emulation’, *Technometrics* **59**(1), 80–92.

O’Hagan, A. (2006), ‘Bayesian analysis of computer code outputs: A tutorial’, *Reliability Engineering & System Safety* **91**(10-11), 1290–1300.

Paterson, J., D’Amico, F., Thies, P., Kurt, R. & Harrison, G. (2018), ‘Offshore wind installation vessels—a comparative assessment for UK offshore rounds 1 and 2’, *Ocean Engineering* **148**, 637–649.

Plumlee, M. & Tuo, R. (2014), ‘Building accurate emulators for stochastic simulations via quantile Kriging’, *Technometrics* **56**(4), 466–473.

Qian, P. Z. & Wu, C. J. (2008), ‘Bayesian hierarchical modeling for integrating low-accuracy and high-accuracy experiments’, *Technometrics* **50**(2), 192–204.

Rasmussen, C. E. (2006), *Gaussian processes for machine learning*, Adaptive computation and machine learning, MIT Press, Cambridge, Mass.

Rocchetta, R., Zio, E. & Patelli, E. (2018), ‘A power-flow emulator approach for resilience assessment of repairable power grids subject to weather-induced failures and data deficiency’, *Applied energy* **210**, 339–350.

Sacks, J., Welch, W. J., Mitchell, T. J. & Wynn, H. P. (1989), ‘Design and analysis of computer experiments’, *Statistical Science* **4**(4), 409–423.

Santner, T. J., Williams, B. J., Notz, W. & Williams, B. J. (2003), *The Design and Analysis of Computer Experiments*, Vol. 1, Springer.

Singh, P., Couckuyt, I., Elsayed, K., Deschrijver, D. & Dhaene, T. (2017), ‘Multi-objective geometry optimization of a gas cyclone using triple-fidelity co-kriging surrogate models’, *Journal of Optimization Theory and Applications* **175**(1), 172–193.

Sudret, B. (2008), 'Global sensitivity analysis using polynomial chaos expansions', *Reliability Engineering & System Safety* **93**(7), 964–979.

Vanhellemont, Q. & Ruddick, K. (2014), 'Turbid wakes associated with offshore wind turbines observed with landsat 8', *Remote Sensing of Environment* **145**, 105–115.

Wilkinson, D. J. (2011), *Stochastic modelling for systems biology, second edition*, Chapman & Hall/CRC Mathematical and Computational Biology, 2nd edn, Taylor and Francis, Hoboken.

Wilson, K. J., Henderson, D. A. & Quigley, J. (2018), 'Emulation of utility functions over a set of permutations: sequencing reliability growth tasks', *Technometrics* **60**(3), 273–285.

Zitrou, A., Bedford, T. & Walls, L. (2016), 'A model for availability growth with application to new generation offshore wind farms', *Reliability Engineering and System Safety* **152**(C), 83–94.

Zitrou, A., Bedford, T., Walls, L., Wilson, K. & Bell, K. (2013), Availability growth and state-of-knowledge uncertainty simulation for offshore wind farms, in '22nd ESREL conference 2013'.

URL: <https://strathprints.strath.ac.uk/45377/>